

## Is the analysis of flow at the CERN Super Proton Synchrotron reliable?

Nicolas Borghini,<sup>1</sup> Phuong Mai Dinh,<sup>2</sup> and Jean-Yves Ollitrault<sup>2</sup>

<sup>1</sup>*Laboratoire de Physique Théorique des Particules Élémentaires, Université Pierre et Marie Curie, 4, place Jussieu, F-75252 Paris Cedex 05, France*

<sup>2</sup>*Service de Physique Théorique, CEA-Saclay, F-91191 Gif-sur-Yvette Cedex, France*

(Received 21 April 2000; published 14 August 2000)

Several heavy ion experiments at SPS have measured azimuthal distributions of particles with respect to the reaction plane. These distributions are deduced from two-particle azimuthal correlations under the assumption that they result solely from correlations with the reaction plane. In this paper, we investigate other sources of azimuthal correlations: transverse momentum conservation, which produces back-to-back correlations, resonance decays such as  $\Delta \rightarrow p\pi$ , HBT correlations, and final state interactions. These correlations increase with impact parameter: most of them vary with the multiplicity  $N$  like  $1/N$ . When they are taken into account, the experimental results of the NA49 Collaboration at SPS are significantly modified. These correlations might also explain an important fraction of the pion directed flow observed by WA98. Data should be reanalyzed taking into account carefully these nonflow correlations.

PACS number(s): 25.75.Ld, 25.75.Gz

### I. INTRODUCTION

In ultrarelativistic heavy ion collisions, azimuthal distributions of the produced particles with respect to the reaction plane are of particular interest. Their anisotropies, which we refer to as “flow,” result from the interactions between the produced particles. They thus probe the hot stages of the collision and may provide valuable information on the state of the interaction region: thermalized or not, equation of state, etc. [1–5]. In the recent years, flow has been measured by many experiments at the Brookhaven AGS with Au projectiles [6–8] and at the CERN SPS with Pb projectiles [9–14]. Since the orientation of the reaction plane is not known *a priori*, flow measurements are usually extracted from two-particle azimuthal correlations. This is based on the idea that azimuthal correlations between two particles are generated by the correlation of the azimuth of each particle with the reaction plane.

The assumption that this is the only source of two-particle azimuthal correlations dates back to the early days of the flow [15]. It still underlies the analyses done at ultrarelativistic energies, both at AGS and at SPS (see, however, [16]). However, there are various sources of direct azimuthal correlations between particles, which do not involve the reaction plane. We have shown in a recent paper [17] that the quantum correlations due to the HBT effect yield azimuthal correlations. When they are taken into account, the results obtained for the charged pion flow by the NA49 Collaboration [9] change significantly. Here, we investigate other sources of nonflow azimuthal correlations. A first source is the condition that the total transverse momentum of the outgoing particles is zero: this gives a back-to-back correlation between their momenta, which can be evaluated quantitatively. This effect is usually taken into account at lower energies [18] but has been neglected so far at AGS and SPS. Other correlations are due to resonance decays such as  $\Delta \rightarrow p\pi$  and  $\rho \rightarrow \pi\pi$ . Finally, Coulomb and strong interactions between pairs of particles with low relative velocities (which we refer

to as “final state interactions”) produce small angle azimuthal correlations [19].

Most of these correlations are typically of order  $1/N$ , where  $N$  is the number of particles emitted in the collision. At SPS energies, correlations due to flow are so small that additional correlations become of the same order, and cannot be neglected. The  $1/N$  dependence also determines the variation of nonflow correlations with the centrality of the collision. Therefore they increase with impact parameter up to very peripheral collisions; on the other hand, they do not vanish for central collisions where the flow is zero by symmetry. They are very important at large impact parameters and should be taken into account, in particular, when studying the centrality dependence of the flow, which has been recently proposed as a sensitive probe of the phase transition to the quark-gluon plasma [20–22].

In Sec. II, we briefly recall how the flow can be extracted from two-particle azimuthal correlations. We use the same method and notations as in [17]. The various sources of nonflow correlations are reviewed and their effects are estimated in Sec. III. The experimental data obtained by the NA49 and WA98 Collaborations for Pb-Pb collisions at SPS are discussed in Sec. IV. We show in particular that the effect of momentum conservation alone is large enough to reverse the sign of the proton directed flow measured by NA49 [9], which is used to define the reaction plane.  $\Delta$  decays produce correlations which are of the opposite sign, and of the same order of magnitude, although we do not attempt to calculate them accurately. For WA98, final state interactions play an important part, and may explain a large fraction of the observed pion directed flow. Our conclusions are given in Sec. V.

### II. TWO-PARTICLE AZIMUTHAL CORRELATIONS AND STANDARD FLOW ANALYSIS

In this section, we define the flow and nonflow contributions to two-particle azimuthal correlations, and we show how azimuthal distributions with respect to the reaction

plane can be extracted from these correlations.

We call ‘‘flow’’ the azimuthal correlations between the outgoing particles and the reaction plane. These are best conveniently characterized in terms of the Fourier coefficients  $v_n$  [23] which we now define. We choose a coordinate system in which the  $x$  axis is the impact direction, and  $(x, z)$  the reaction plane.  $\phi$  denotes the azimuthal angle with respect to the reaction plane. In this frame,  $v_n$  can be expressed as a function of the one-particle momentum distribution  $dN_j/d^3\mathbf{p}$  for a particle of type  $j$  (in this paper, we consider pions and protons):

$$v_n(p_T, y, j) \equiv \langle \cos n\phi \rangle = \frac{\int_0^{2\pi} \cos n\phi \frac{dN_j}{d^3\mathbf{p}} d\phi}{\int_0^{2\pi} \frac{dN_j}{d^3\mathbf{p}} d\phi}, \quad (1)$$

where the brackets denote an average value over many events with approximately the same impact parameter, and  $p_T$  and  $y$  are the transverse momentum and rapidity of the particle. Since the system is symmetric with respect to the reaction plane for spherical nuclei,  $\langle \sin n\phi \rangle$  vanishes. The goal of the flow analysis is to extract  $v_n$  from the data. The coefficients  $v_1$  and  $v_2$  are usually called directed and elliptic flow, respectively [24].

Since the reaction plane is not known experimentally, one can only measure relative azimuthal angles between the outgoing particles. In particular, one measures the Fourier coefficients of the relative azimuthal distribution between two species of particles  $j$  and  $k$

$$\begin{aligned} c_n^{\text{measured}}(p_{T1}, y_1, j; p_{T2}, y_2, k) & \equiv \langle \cos n(\phi_1 - \phi_2) \rangle \\ & = \frac{\int \int \cos n(\phi_1 - \phi_2) \frac{dN_{jk}}{d^3\mathbf{p}_1 d^3\mathbf{p}_2} d\phi_1 d\phi_2}{\int \int \frac{dN_{jk}}{d^3\mathbf{p}_1 d^3\mathbf{p}_2} d\phi_1 d\phi_2}. \end{aligned} \quad (2)$$

The two-particle distribution can generally be expressed as the sum of an uncorrelated distribution and two-particle correlations:

$$\frac{dN_{jk}}{d^3\mathbf{p}_1 d^3\mathbf{p}_2} = \frac{dN_j}{d^3\mathbf{p}_1} \frac{dN_k}{d^3\mathbf{p}_2} [1 + C_{jk}(\mathbf{p}_1, \mathbf{p}_2)], \quad (3)$$

where  $C_{jk}(\mathbf{p}_1, \mathbf{p}_2)$  is the two-particle connected correlation function. Using this decomposition, one can write  $c_n^{\text{measured}}$  as the sum of two terms:

$$\begin{aligned} c_n^{\text{measured}}(p_{T1}, y_1, j; p_{T2}, y_2, k) & = c_n^{\text{flow}}(p_{T1}, y_1, j; p_{T2}, y_2, k) \\ & + c_n^{\text{nonflow}}(p_{T1}, y_1, j; p_{T2}, y_2, k), \end{aligned} \quad (4)$$

where the first term is due to flow:

$$c_n^{\text{flow}}(p_{T1}, y_1, j; p_{T2}, y_2, k) = v_n(p_{T1}, y_1, j) v_n(p_{T2}, y_2, k), \quad (5)$$

while the remaining term comes from direct two-particle correlations:

$$\begin{aligned} c_n^{\text{nonflow}}(p_{T1}, y_1, j; p_{T2}, y_2, k) & = \frac{\int \int \cos n(\phi_1 - \phi_2) C_{jk}(\mathbf{p}_1, \mathbf{p}_2) \frac{dN_j}{d^3\mathbf{p}_1} \frac{dN_k}{d^3\mathbf{p}_2} d\phi_1 d\phi_2}{\int \int \frac{dN_{jk}}{d^3\mathbf{p}_1 d^3\mathbf{p}_2} d\phi_1 d\phi_2}. \end{aligned} \quad (6)$$

From the flow term (5), one can calculate the Fourier coefficient  $v_n$ , up to a sign (see [17] for details):

$$v_n(p_T, y, j) = \pm \frac{c_n^{\text{flow}}(p_T, y, j; \mathcal{D})}{\sqrt{c_n^{\text{flow}}(\mathcal{D}; \mathcal{D})}}, \quad (7)$$

where  $\mathcal{D}$  denotes the detector used to estimate the reaction plane,  $c_n(p_{T1}, y_1, j; \mathcal{D})$  the average value of  $c_n$  over  $(p_{T2}, y_2, k)$  in  $\mathcal{D}$ , and  $c_n(\mathcal{D}; \mathcal{D})$  the average over both  $(p_{T1}, y_1, j)$  and  $(p_{T2}, y_2, k)$ .

Experimental analyses usually assume that the only azimuthal correlation between outgoing particles is due to their correlation with the reaction plane, i.e., they neglect  $c_n^{\text{nonflow}}$ . This means that the published flow data are given by Eq. (7) with  $c_n^{\text{flow}}$  replaced by the total correlation  $c_n^{\text{measured}}$ ; in turn, the total correlation can be reconstructed from the published flow data using Eq. (5).

We shall see in Sec. III that  $c_n^{\text{nonflow}}$  is typically of order  $1/N$  where  $N$  denotes the number of outgoing particles. In a central Pb-Pb collision at SPS,  $N \sim 2500$ , so that one expects  $c_n^{\text{nonflow}} \sim 4 \times 10^{-4}$ . This is certainly a weak effect. However, the total azimuthal correlation is also weak: since the directed and elliptic flow at SPS measured by NA49 are of the order of 3% [9], one obtains from Eq. (5) (since it is assumed that all the measured correlation is from flow)  $c_n^{\text{measured}} \sim 9 \times 10^{-4}$ , only a factor of 2 larger than nonflow correlations. Therefore one cannot neglect the latter. In order to take them into account, one must estimate the various contributions to  $c_n^{\text{nonflow}}$ , subtract them from  $c_n^{\text{measured}}$  in Eq. (4) to isolate  $c_n^{\text{flow}}$ , and calculate the resulting  $v_n$  using Eq. (7). In [17], we applied this procedure to the NA49 data on pion flow [9], taking into account correlations due to the HBT effect. In Sec. IV, we consider in addition the effects of momentum conservation and resonance decays.

### III. SOURCES OF NONFLOW CORRELATIONS

Several physical effects yield two-particle correlations, which contribute to the nonflow correlation defined in Eq. (6). In this section, we discuss momentum conservation, resonance decays, quantum HBT correlations, and final state interactions, and we estimate their respective contributions to  $c_n^{\text{nonflow}}$ .

### A. Transverse momentum conservation

Global momentum conservation gives a back-to-back correlation between the produced particles. Since we are interested in azimuthal correlations, we consider only transverse momentum. Its contribution to  $C_{jk}(\mathbf{p}_1, \mathbf{p}_2)$ , which we denote by  $C_{jk}^{\Sigma p_T}(\mathbf{p}_1, \mathbf{p}_2)$ , is calculated in Appendix A in the case where there is no other correlation between particles. The result is

$$C_{jk}^{\Sigma p_T}(\mathbf{p}_1, \mathbf{p}_2) = - \frac{2\mathbf{p}_{T1} \cdot \mathbf{p}_{T2}}{\left\langle \sum p_T^2 \right\rangle}, \quad (8)$$

where the sum in the denominator runs over all the particles emitted in the collision. This correlation is clearly of order  $1/N$ . The Fourier coefficient  $c_n^{\Sigma p_T}$  is obtained by inserting Eq. (8) in Eq. (6). Neglecting azimuthal anisotropies of the one-particle distribution, which are of the order of a few percent [9], one finds a result which is nonvanishing only for  $n=1$ :

$$c_1^{\Sigma p_T}(p_{T1}, y_1, j; p_{T2}, y_2, k) = - \frac{p_{T1} p_{T2}}{\left\langle \sum p_T^2 \right\rangle}. \quad (9)$$

Since  $c_n^{\Sigma p_T}$  vanishes for  $n \neq 1$ , the effects of momentum conservation must be taken into account only in the measurement of directed flow. Equation (9) allows us to calculate the correlation arising from momentum conservation, as soon as the value of the denominator  $\langle \sum p_T^2 \rangle$  is known. This quantity is evaluated in Appendix B in the case of Pb-Pb collisions at SPS. The value (B3) is probably overestimated, which means that we underestimate the correction due to momentum conservation in the numerical calculations of Sec. IV. Equation (9) shows that the azimuthal correlations between two particles due to momentum conservation are independent of the rapidities  $y_1$  and  $y_2$  and of the particle species  $j$  and  $k$ , but increase linearly with transverse momentum. The effect is therefore stronger for heavier particles, which have larger transverse momenta, as for instance protons. The centrality dependence is also easily determined: since transverse momentum spectra depend weakly on the centrality [25,26],  $\langle \sum p_T^2 \rangle$  scales like the multiplicity  $N$ , so that  $c_1^{\Sigma p_T}$  scales like  $1/N$ . Note, finally, that momentum conservation does not contribute if the window used for the reaction plane determination is symmetric around midrapidity [18].

### B. Resonance decays

We now discuss the azimuthal correlation between the decay products of a resonance. It is known that many pions originate from  $\rho \rightarrow \pi\pi$  decays, and that many nucleons are excited into  $\Delta$  resonances [27,28], which then decay into a nucleon and a pion. When pions are used to determine the reaction plane,  $\rho$  (respectively  $\Delta$ ) decays must be taken into account in the analysis of the pion (respectively proton) flow; when protons are used,  $\Delta$  decays must be taken into account

in the analysis of the pion flow. Resonances with higher masses are less abundant and will not be considered in this paper; however, they may also give rise to sizeable correlations.

The contribution of a resonance decay, say,  $\Delta \rightarrow p\pi$ , to  $c_n^{\text{nonflow}}$  is the product of two factors: the first factor is the average value of  $\cos n(\phi_1 - \phi_2)$  where  $\phi_1$  and  $\phi_2$  are the azimuthal angles of a proton and a pion originating from the same  $\Delta$ ; the second factor is the probability that a given proton and a given pion originate from the same  $\Delta$ . This probability is hard to estimate. There are recent measurements of  $\rho^0$  [29] and  $\Delta^{++}$  [27] multiplicities, but this is not sufficient: indeed, due to the short resonance lifetimes, the decay products may interact again after they have been produced, in a way which depends on the detailed collision dynamics. Microscopic models of heavy ion collisions (see [30] for a review) could be used to calculate correlations from resonance decays, but the discussion in this paper will remain at a more qualitative level.

Generally, in a two-particle decay, the azimuthal correlation depends on the relative magnitude of the velocity  $V$  of the decaying particle and the velocities  $V_1$  and  $V_2$  of the products in the rest frame of the decaying particle: in particular, the azimuthal angles of the decay products are equal ( $\phi_1 = \phi_2$ ) in the limit where  $V_1 = V_2 = 0$ , while they are back-to-back ( $\phi_1 = \phi_2 + \pi$ ) if  $V = 0$ . This is illustrated in Fig. 1, which displays the average value of  $\langle \cos(\phi_1 - \phi_2) \rangle$  and  $\langle \cos 2(\phi_1 - \phi_2) \rangle$  for the decays  $\Delta \rightarrow p\pi$  and  $\rho \rightarrow \pi\pi$ , as functions of the transverse momentum of the decaying resonance. Assuming that the transverse momentum distribution is exponential in the transverse mass  $m_T = \sqrt{p_T^2 + m^2}$ , i.e.,  $dN/d^2\mathbf{p}_T \propto \exp(-m_T/T)$  [see Eq. (B1)], one can average the correlations displayed in Fig. 1 over  $p_T$ . The result is shown in Fig. 2, as a function of the inverse slope parameter  $T$ . Taking for  $\Delta$  the same value of  $T$  as for protons, i.e.,  $T \approx 300$  MeV, one sees that the contribution to  $c_1$  is large and positive, while the contribution to  $c_2$  is close to zero. In the case of  $\rho$  decays, assuming that  $T$  varies linearly with the mass [31] one may choose  $T \approx 270$  MeV, which results in both  $c_1$  and  $c_2$  slightly negative.

In order to obtain the contribution of  $\Delta$  decays to  $c_n^{\text{nonflow}}$ , one must multiply the correlation displayed in Fig. 1 by the probability  $p_\Delta$  that a given pion and a given proton originate from the same  $\Delta$ , as explained above. Let  $\alpha$  denote the fraction of nucleons are excited into  $\Delta$  resonances. Then, the probability  $p_\Delta$  is  $\alpha/N_\pi$  where  $N_\pi$  is the number of pions. From isospin symmetry, one expects this probability to be the same for neutral and charged pions. Since most particles are pions,  $N_\pi \sim N$ . If  $\alpha$  is of order unity, we obtain finally  $c_n^{\Delta \rightarrow p\pi} \sim 1/N$ . The centrality dependence of this correlation is also in  $1/N$  if the relative abundance of  $\Delta$  is independent of centrality. Similar arguments hold for the correlations due to  $\rho$  decays.

Note that a way to eliminate correlations from  $\Delta$  decays experimentally would be to measure protons and pions in widely separated rapidity windows. Indeed, the maximum rapidity difference between the decay products of a  $\Delta$  is 1.5. In the case of the  $\rho \rightarrow \pi\pi$  decay, the maximum rapidity dif-

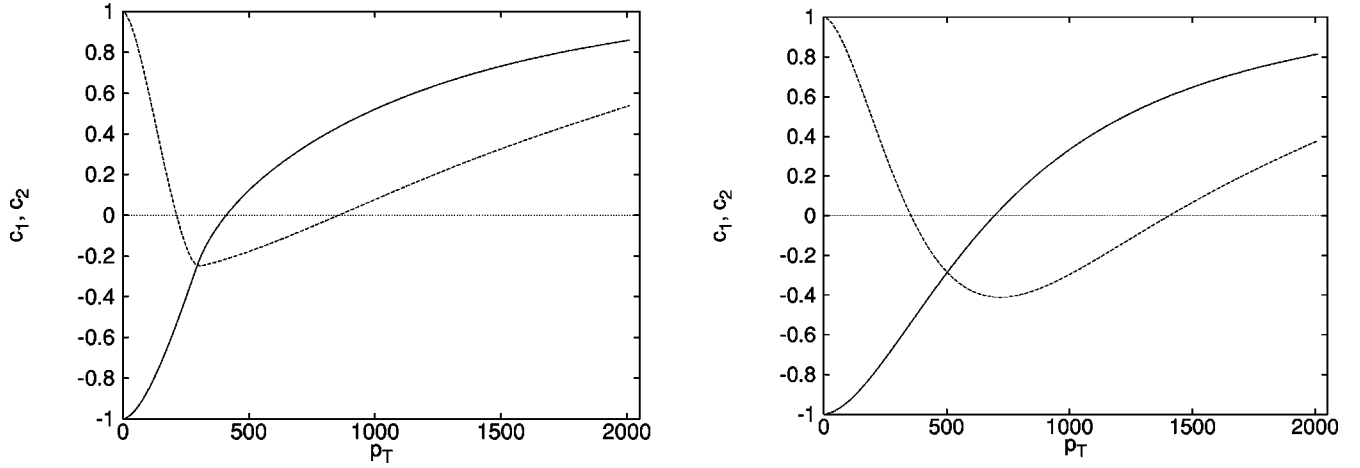


FIG. 1. Average value of  $\cos(\phi_1 - \phi_2)$  (full curve) and  $\cos 2(\phi_1 - \phi_2)$  (dashed curve), where  $\phi_1$  and  $\phi_2$  are the azimuthal angles of the decay products of  $\Delta \rightarrow p\pi$  (left) or  $\rho \rightarrow \pi\pi$  (right), as a function of the transverse momentum of the decaying particle in MeV/c.

ference between the outgoing pions is 3.3, so that the corresponding correlation is harder to eliminate.

### C. Small angle correlations

Finally, there are correlations between particles with low relative velocities: quantum HBT correlations between identical particles, Coulomb interactions between charged particles, and strong interactions.

Azimuthal correlations between identical particles due to the HBT effect were studied in detail in [17]. The Fourier coefficient  $c_n^{\text{HBT}}(\mathbf{p}_1, \mathbf{p}_2)$  is of order unity if the relative momentum  $|\mathbf{p}_1 - \mathbf{p}_2|$  is smaller than  $\hbar/R$ , where  $R$  is the size of the particle source. It depends weakly on  $n$ . The order of magnitude of  $c_n^{\text{HBT}}$  integrated over phase space is therefore  $c_n^{\text{HBT}} \sim (\hbar/Rp)^3$ , where  $p$  denotes a typical momentum. In the case of a high temperature massless pion gas,  $p$  is of order  $T/c$ , while the particle density  $N/R^3$  is of order  $(T/\hbar c)^3$ , so that  $c_n^{\text{HBT}}$  is again of order  $1/N$  [32]. One would expect the centrality dependence of  $c_n^{\text{HBT}}$  to follow the same behavior. However, the measured HBT radii vary more

slowly than  $N^{1/3}$  [33]. In collisions with sulphur projectiles, a dependence in  $R \propto N^\alpha$  was found with  $\alpha \approx 0.2$  [34]. If the same behavior holds for Pb-Pb collisions, the dependence of azimuthal HBT correlations with centrality will be in  $N^{-0.6}$ . Finally,  $c_n^{\text{HBT}}(\mathcal{D})$  is proportional to the one-particle momentum distribution, hence it is larger at low  $p_T$ .

More generally, all particles with low relative velocities undergo final state interactions, strong and/or electrostatic [19]. One defines the invariant momentum as  $Q_{\text{inv}} = 2\mu v_{\text{rel}}$ , where  $\mu = m_1 m_2 / (m_1 + m_2)$  is the reduced mass and  $v_{\text{rel}} = \sqrt{1 - m_1^2 m_2^2 / (P_1 \cdot P_2)^2}$  is the relative velocity of the two particles with four-momenta  $P_1$  and  $P_2$ . Then the correlations due to strong interactions are sizeable only in a limited  $Q_{\text{inv}}$  range, independent of the size of the interaction region. For instance, proton-proton correlations, which are dominated by strong interactions, are maximum for  $Q_{\text{inv}} \approx 20$  MeV/c, and negligible for  $Q_{\text{inv}} \geq 40$  MeV/c, for any projectile and target [35]. On the other hand, the range over which Coulomb correlations are significant depends on the system size. For Pb-Pb collisions at SPS,  $p$ - $\pi^+$  correlations,

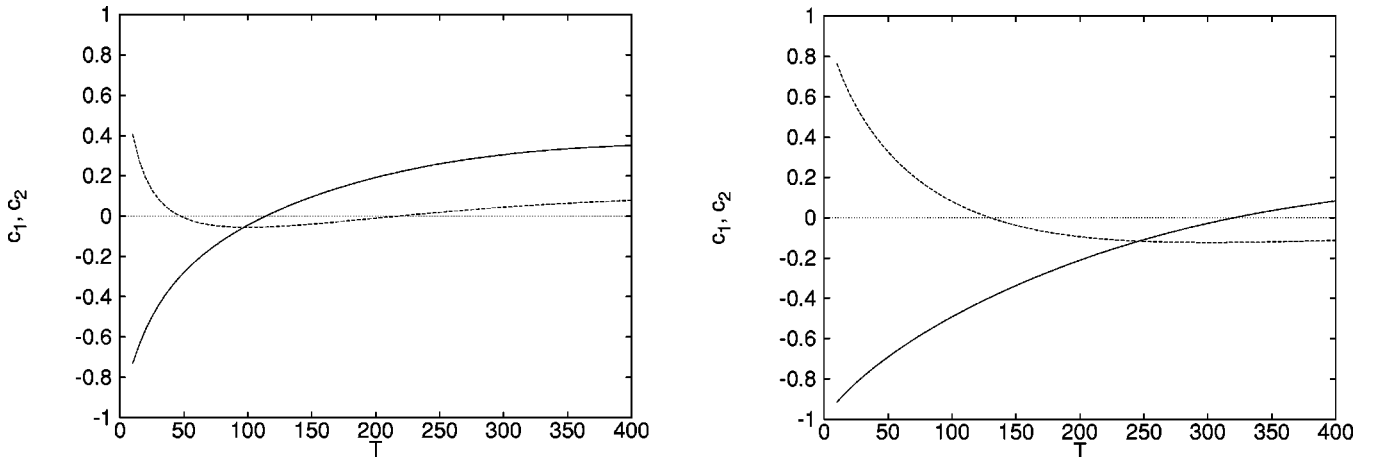


FIG. 2. Same as Fig. 1, as a function of the inverse slope parameter  $T$  of the resonance distribution in MeV. Left:  $\Delta \rightarrow p\pi$ ; right:  $\rho \rightarrow \pi\pi$ .

TABLE I. Properties of the various sources of two-particle azimuthal correlations.

	Momentum conservation	Resonance decays	Small angle correlations
Which pairs?	any	$ y_1 - y_2  < 1.5$ ( $\Delta$ ) $ y_1 - y_2  < 3.3$ ( $\rho$ )	low relative velocities identical particles (HBT)
$n$ dependence	$n = 1$ only	nontrivial	weak
centrality dependence	$1/N$	$1/N$	$1/N^{0.6?}$ (HBT) $1/N$ (strong) $1/N^{1/3?}$ (Coulomb)
$p_T$ range	high $p_T$	nontrivial	low $p_T$
under control?	calculated	simulations, microscopic models	measured

which are dominated by the Coulomb repulsion, extend up to  $Q_{\text{inv}} \approx 50$  MeV/c [36]. Both Coulomb and strong interactions give rise to small angle azimuthal correlations, similar to those due to the HBT effect. Thus the resulting contribution to  $c_n^{\text{nonflow}}$ , denoted by  $c_n^{\text{FSI}}$ , is expected to be weakly dependent on the order  $n$  of the Fourier component, and  $c_n^{\text{FSI}}(p_T, y, \mathcal{D})$  is roughly proportional to the one-particle distribution.

The centrality dependence differs for Coulomb and strong interactions. For strong interactions, the strength of the correlation at a given  $Q_{\text{inv}}$  varies like  $1/V$ , where  $V$  is the volume of the system [19]. This is due to the fact that the range of the interaction is much smaller than the size of the system. Thus the centrality dependence follows a  $1/N$  behavior. For Coulomb interactions, which are long-ranged, the  $N$  dependence is weaker. We do not attempt to evaluate this dependence. By analogy with the Coulomb potential, it might vary like  $1/L$ , with  $L$  the size of the interaction region, i.e., like  $1/N^{1/3}$ .

Both HBT and final state interactions can be eliminated by studying the correlation between particles widely separated in phase space, so that their invariant relative momentum is much larger than, typically, 50 MeV/c.

#### D. Summary

The properties of the three main types of two-particle correlations studied above are summarized in Table I. Note that while the average over all phase space of the three is of order  $1/N$ , they can be much larger in definite regions of phase space, for example at low relative momentum for HBT correlations. Note also that this catalogue of two-particle correlations may not be exhaustive.

As we have seen, two-particle correlations are generally of order  $1/N$ , much smaller than unity. We therefore assume that the contributions of the various effects can simply be added. If one studies the correlation between identical pions, for instance, there are contributions to  $c_n^{\text{nonflow}}$  from momentum conservation, denoted by  $c_n^{\Sigma p_T}$ , from  $\rho \rightarrow \pi\pi$  decays, denoted by  $c_n^\rho$ , from HBT correlations, denoted by  $c_n^{\text{HBT}}$ , and from final state interactions, denoted by  $c_n^{\text{FSI}}$ . The resulting nonflow correlation is

$$c_n^{\text{nonflow}} = c_n^{\Sigma p_T} + c_n^\rho + c_n^{\text{HBT}} + c_n^{\text{FSI}}. \quad (10)$$

## IV. APPLICATION TO SPS DATA

The most detailed flow analyses in Pb-Pb collisions at SPS were performed by the NA49 and WA98 Collaborations. NA49 estimates the reaction plane using pions in the forward hemisphere, while WA98 uses protons and fragments close to the target rapidity. In this section, we discuss to what extent nonflow correlations may contribute to the measured azimuthal correlations, which are assumed to be solely due to flow in both experiments. In the case of the NA49 data, we shall explicitly subtract the various nonflow correlations, following the method outlined in Sec. II, and see what the ‘‘true’’ flow might be. Our discussion of WA98 data will remain at a semiquantitative level due to the complex acceptance of the Plastic Ball detector used for the flow analysis.

### A. NA49 data

The NA49 experiment at CERN measures the directed and elliptic flow of pions and protons in Pb-Pb collisions at 158 GeV per nucleon [9]. Charged pions are used to estimate the reaction plane, in the kinematic window  $4 < y < 6$  and  $0 < p_T < 600$  MeV/c for directed flow,  $3.5 < y < 5$  and  $0 < p_T < 2000$  MeV/c for elliptic flow [37]. The azimuthal distribution of identified particles (protons and charged pions) is then measured with respect to this reaction plane. We now show the effect of taking into account the various sources of nonflow correlations discussed in the previous section.

We begin with the directed flow of protons. It is obtained from from Eq. (7), where  $\mathcal{D}$  refers to charged pions in the above mentioned kinematic window. The numerator in this equation corresponds to the correlations between protons and the pions in  $\mathcal{D}$ , while the denominator corresponds to the correlations between the pions in  $\mathcal{D}$ . The arbitrary sign in Eq. (7) is chosen negative by NA49, in order to obtain a positive  $v_1$  for protons (see Fig. 3), as usually assumed at high energies in the forward rapidity region [15].

The correction to the denominator in Eq. (7) from nonflow correlations will be discussed below, when we discuss the pion flow. It is a small correction, of a few percent. The numerator of Eq. (7) gets contributions from momentum conservation,  $\Delta \rightarrow p\pi$  decays, and final state interactions.

We first discuss momentum conservation. The corresponding azimuthal correlation is given by Eqs. (9) and (B3). Since it is negative, once it is subtracted from the measured

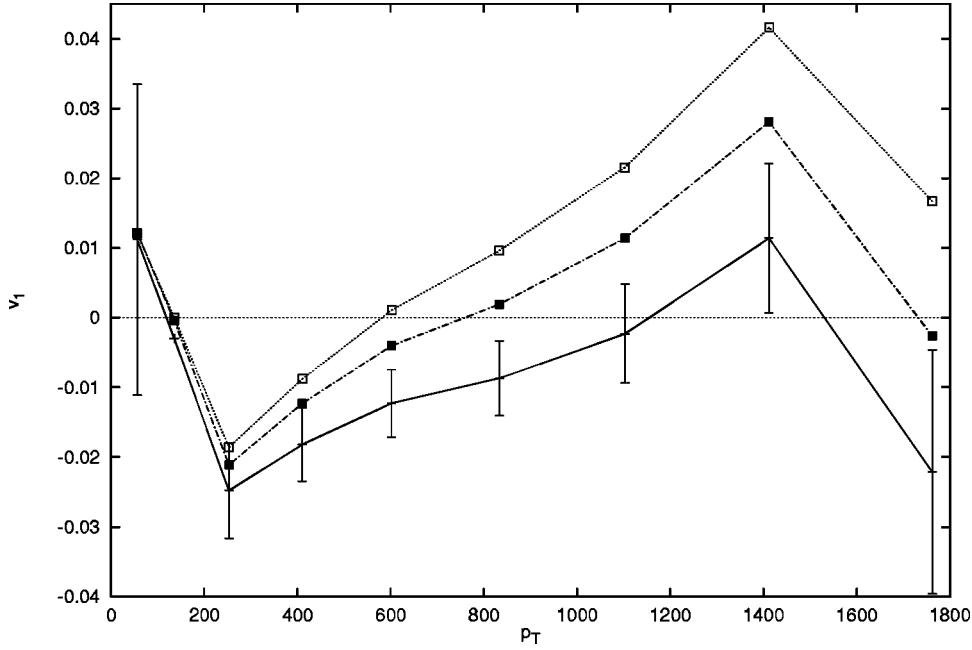


FIG. 3. Directed flow  $v_1$  of protons, integrated over the range  $3 < y < 6$ , as a function of the transverse momentum  $p_T$ , measured by NA49 (open squares), taking into account momentum conservation only (with error bars), and with a simulation of correlations from  $\Delta$  decays (filled squares). Error bars are taken from experiment.

correlation (4), this gives a positive correction to the correlations due to flow  $c_1^{\text{flow}}$ . Because of the negative sign in Eq. (7), the correction to  $v_1$  is finally negative. As can be seen in Fig. 3, the correction is so large that the sign of the proton directed flow is now negative for almost all  $p_T$ . Now, the sign of the proton directed flow is particularly important since it is used to fix the arbitrary sign in Eq. (7), which is chosen so that  $v_1 > 0$  in the forward rapidity region for protons. The surprising result is that the directed flows of pions and protons now have the same sign. This is contrary to the theoretical expectation that nucleons and pions flow in opposite directions, because of pion rescattering [38,39], and to other measurements at AGS [6] and at SPS [10].

Since the correlation between pions and protons from  $\Delta \rightarrow p\pi$  decays is positive (see Fig. 2), it may restore the original sign of the proton directed flow  $v_1$ . As explained in the previous section, an accurate computation of this correlation would require a microscopic model. We present in Fig. 3 a crude estimate of the effect, based on a simple Monte Carlo calculation taking into account the acceptance windows of NA49 for protons and pions. We do not take into account the possible rescatterings of the decay products. Our assumptions are the following: 50% of the outgoing protons originate from  $\Delta$  decays, as suggested by simulations based on the UrQMD model [28]. We take into account the fact that only 2/3 of  $\Delta$  decays yield a charged pion. The mass distribution of  $\Delta$ 's follows a Lorentzian, their rapidity distribution is flat between 0 and 5.8 (i.e., between the target and projectile rapidities), and their transverse momentum distribution is exponential in  $m_T$  [see Eq. (B1)] with an inverse slope parameter  $T = 300$  MeV, as for protons. One sees in Fig. 3 that correlations from  $\Delta$  decays can indeed restore the positive sign for the proton directed flow, since their contribution is almost as large as that from momentum conservation in absolute value.

In principle, one should also take into account final state interactions. Since the pions used to determine the reaction

plane are approximately half  $\pi^+$  and half  $\pi^-$ , Coulomb effects cancel. Correlations between pions and protons due to strong interactions are small and should not contribute significantly to  $c_n^{\text{measured}}$ .

We now turn to the directed flow of charged pions. Since pions are also used to estimate the reaction plane, pion-pion correlations are involved in both the numerator and the denominator of Eq. (7). Following Eq. (10), we must take into account momentum conservation,  $\rho$  decays, the HBT effect, and final state interactions. We neglect final state interactions for the same reasons as for protons. According to Fig. 2, the correlation from  $\rho$  decay is small. We also neglect it. Three sets of points are displayed in Fig. 4: NA49 data without correction, with correction for HBT correlations (taken from [17]) and with correction for HBT and momentum conservation. While the correction due to the HBT effect is important at low  $p_T$ , momentum conservation changes the pion flow at high  $p_T$ ; the latter effect is less important than for protons, because pions have lower transverse momenta. However, the positive pion flow observed by NA49 at high  $p_T$  seems to be explained by momentum conservation.

Let us say a few words about elliptic flow. Here, momentum conservation does not contribute, as discussed in the previous section. For protons,  $\Delta$  decays probably give a negligible contribution to  $c_2^{\text{measured}}$ , as explained in Sec. III B. For pions, HBT correlations significantly reduce elliptic flow at low  $p_T$ , as shown in [17]. Here,  $\rho$  decays should be taken into account. As discussed in Sec. III B, they give a negative correlation, i.e., opposite to the correlation due to flow. Therefore, taking  $\rho$  decays into account would lead to a (slight) increase of the pion  $v_2$ .

Finally, the centrality dependence of the directed and elliptic flow of pions has been studied recently [40]. It is striking to note that both increase continuously as the reaction becomes more peripheral, which is the behavior expected for nonflow correlations. We have shown that at least a fraction

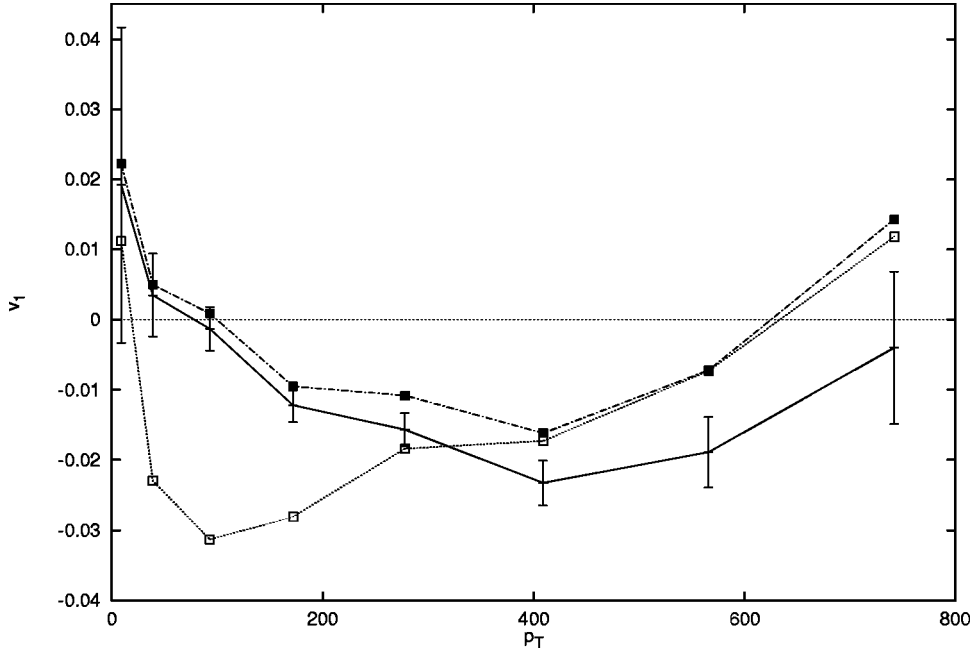


FIG. 4. Directed flow  $v_1$  of pions, integrated between  $4 < y < 5$ , as a function of the transverse momentum  $p_T$  in MeV/c, measured by NA49 (open squares), after subtraction of HBT correlations (filled squares), and after subtraction of both HBT and transverse momentum conservation correlations (with error bars).

of the measured correlation, which is interpreted as flow, is due to nonflow correlations. Even if it is only a small fraction, it will increase with impact parameter and eventually dominate for the most peripheral collisions. It is thus likely that the measurements of flow at large impact parameter are contaminated by nonflow phenomena. However, none of the above mechanisms can explain the observed  $y$  dependence of directed flow, which increases (in absolute value) up to the projectile rapidity for peripheral collisions.

### B. WA98 data

We shall now discuss the results obtained by the WA98 experiment at CERN for the directed flow of protons and positive pions [10]. There, the reaction plane is estimated using protons and fragments detected by the Plastic Ball, in the target rapidity region  $-0.6 < y < 0.3$ . One then measures the azimuthal angle of a positive pion or a proton detected in the Plastic Ball with respect to this estimated plane. If the particle is a proton, it is not used in the determination of the reaction plane to avoid autocorrelations. Two points closer to midrapidity are obtained using the tracking system, for which the flow is zero within error bars; we shall not consider these two points here. Contrary to the NA49 analysis where pions were used to estimate the reaction plane, the flow of protons (respectively pions) is now determined from proton-proton (respectively pion-proton) azimuthal correlations. The value of  $v_1$  is still obtained from Eq. (7), where the arbitrary sign is again chosen negative, so that the directed flow of protons be negative, as it should in the backward rapidity region. On the other hand, the directed flow of pions is positive, i.e., pions flow opposite to the protons.

WA98 measures the directed flow  $v_1$  in the target fragmentation region. Since  $v_1$  vanishes at midrapidity, it is expected to be larger there than in the more central rapidity region, where NA49 is working. Indeed, the measured values of  $v_1$  are larger for WA98 than for NA49. For semicentral

collisions,  $|v_1|$  is about 0.1 for both pions and protons. Following Eq. (5), this corresponds to an azimuthal correlation  $|c_1^{\text{measured}}| \sim 10^{-2}$ , either between pions and protons or between protons, an order of magnitude larger than for NA49.

The values of  $v_1$  are measured as a function of centrality. For protons,  $-v_1$  reaches a maximum of 0.12 for an impact parameter  $b \sim 8$  fm, while for pions  $v_1$  increases with  $b$  up to very peripheral collisions, where it reaches values as high as 0.3. The latter centrality dependence is reminiscent of the  $1/N$  behavior of nonflow correlations, which suggests that part of the measured flow is spurious. We thus review the various nonflow correlations listed in Sec. III to evaluate their contributions. We shall see that final state interactions are the only significant ones, and that they may explain the pion flow at large impact parameter.

Momentum conservation is less important than for the NA49 experiment. The reason is that the particles detected in the Plastic Ball have low transverse momenta [41]. For protons,  $p_T$  is typically 400 MeV, resulting in  $c_1^{\Sigma p_T}$  of the order of  $-4 \times 10^{-4}$  for the proton-proton correlation, following Eq. (9). This is much smaller than  $c_1^{\text{measured}} \sim 10^{-2}$ . For pions, transverse momenta are even smaller. In both cases, the contribution of transverse momentum conservation to  $c_1^{\text{nonflow}}$  is negligible.

Resonance decays will contribute to the pion flow. The sign of the correlation due to  $\Delta \rightarrow p \pi$  depends on the inverse slope parameter  $T$ , as can be seen in Fig. 2. This quantity is smaller in the fragmentation region than in the central rapidity region, but probably still larger than 100 MeV. Then, the corresponding pion-proton correlation should be positive. It is thus opposite to the correlation measured by WA98, and cannot explain the observed pion flow.

Finally, let us discuss the small angle correlations due to the HBT effect and final state interactions. We shall first summarize the results obtained by the NA49 experiment for two-particle small angle correlations in the central rapidity

region. Then we extrapolate these results to the fragmentation region covered by the WA98 Plastic Ball in order to discuss the correlations measured by WA98.

The NA49 Collaboration has measured both proton-proton [42] and proton- $\pi^+$  [36] small angle correlations for central collisions. Two-proton correlations, resulting from the interplay of the HBT effect and strong and Coulomb interactions, were found to be positive, which means that they are dominated by the attractive strong interaction. They peak at a relative momentum between particles of 20 MeV/c, where they reach 25%, and are no longer significant as soon as  $|\mathbf{p}_1 - \mathbf{p}_2| > 40$  MeV/c. Small angle correlations between positive pions and protons are negative, and typically of the order of  $-10\%$  for invariant momenta smaller than 40 MeV/c, i.e.,  $|\mathbf{p}_{T\pi} - (m_\pi/m_p)\mathbf{p}_{Tp}| < 40$  MeV/c and  $y_\pi - y_p < 40/m_\pi \approx 0.3$ .

Extrapolating these results to the fragmentation region, we can estimate the azimuthal correlation  $c_1^{\text{FSI}}$  for WA98. In the case of proton-proton correlations, we need to evaluate the fraction of proton pairs having relative momenta less than 40 MeV/c, i.e., with  $|\mathbf{p}_{T1} - \mathbf{p}_{T2}| < \Delta p = 40$  MeV/c, and  $y_1 - y_2 < \Delta p/m_T \approx 0.04$ , with  $m_T \approx 1000$  MeV. Since the acceptance window is typically [41]  $p_T^{\text{min}} = 200 < p_T < p_T^{\text{max}} = 600$  MeV/c and  $y^{\text{min}} = -0.4 < y < y^{\text{max}} = 0.1$ , this fraction is

$$\frac{\frac{4\pi}{3}\Delta p^3}{\pi(p_T^{\text{max}2} - p_T^{\text{min}2})m_T(y^{\text{max}} - y^{\text{min}})} \sim 5 \times 10^{-4}. \quad (11)$$

With a correlation strength of 20%, this yields a value of  $c_1^{\text{FSI}}$  of the order of  $10^{-4}$ , much smaller than the measured correlation  $c_1^{\text{measured}}$ . Thus, the measurement of the proton flow is not influenced by small angle correlations.

In the case of pion-proton correlations, we first note that the velocity windows of pions and protons of the WA98 Plastic Ball overlap [41], so that small angle correlations between pions and protons should be taken into account. In fact, the rapidity range is almost the same for pions and protons, while the transverse momentum range is roughly scaled by a factor  $m_\pi/m_p$ , so that the acceptance windows roughly coincide in velocity space. Then, for a given pion, the probability that a proton seen in the Plastic Ball has an invariant relative momentum  $|\mathbf{p}_{T\pi} - (m_\pi/m_p)\mathbf{p}_{Tp}| < \Delta p = 40$  MeV/c is given by Eq. (11) with  $\Delta p$  replaced by  $(m_p/m_\pi)\Delta p$ . This gives a factor  $(m_p/m_\pi)^3 \approx 200$ , compared to Eq. (11), so that the fraction is of the order of  $10^{-1}$ . Using the correlation strength measured by NA49, this gives a correlation  $c_1^{\text{FSI}}(\mathcal{D})$  of order  $-10^{-2}$ , comparable to the measured correlation. On the one hand, this value is overestimated since the acceptance windows for pions and protons do not exactly coincide in velocity space. On the other hand, it is underestimated because the correlations are measured by NA49 for central collisions, and they are even stronger for peripheral collisions. Therefore it is likely that a large fraction of the  $\pi^+$  directed flow seen by WA98 is due to the repulsive Coulomb interaction between positive pions and protons.

## V. DISCUSSION

We have shown that the assumption that all azimuthal correlations between particles are due to flow is no longer valid at SPS energies, where other sources of correlations become of the same order of magnitude due to the smallness of the flow. All the effects studied above, momentum conservation, resonance decays, HBT correlations, final state interactions, turn out to give important correlations. In particular, we have shown that the effect of momentum conservation is so large that it changes the sign of the proton directed flow measured by NA49: this sign is particularly important since it is used to define the orientation of the reaction plane.

The methods currently used to analyze the flow can be modified in order to take into account these additional correlations and to subtract them from the measured correlations, as explained in Sec. II. Correlations from momentum conservation can be calculated. They are governed by only one unknown quantity, the sum over all particles of squared transverse momenta  $\langle \Sigma p_T^2 \rangle$ . Correlations from the decays of short-lived resonances cannot be evaluated so easily. In this paper, we have only given semiquantitative estimates. More accurate calculations would require a microscopic model of the collision. Finally, correlations which affect particles with low relative velocities, i.e., those due to the HBT effect and to final state (Coulomb, strong) interactions can either be measured independently, or eliminated by measuring correlations between particles in widely separated rapidity and/or transverse velocity windows.

However, our list of correlations may not be exhaustive, and one cannot exclude that other sources exist which are of the same order of magnitude as those studied here. There is no systematic way to separate the flow and the nonflow contribution to the measured azimuthal correlation (4). One could try to use the factorization property of Eq. (5) to isolate the correlation due to flow. However, nonflow correlations may also factorize, as is the case for the correlation due to momentum conservation (9).

A way to circumvent these difficulties would be to use the remarkable property of two-particle correlations, that they vary with the multiplicity  $N$  like  $1/N$  (with the possible exception of Coulomb interactions and, to a lesser extent, HBT correlations). This fact has been noted in Sec. III for the various correlations studied, but holds more generally for any extensive system, and would probably still be true for other types of correlations than those listed in Sec. III. This  $1/N$  behavior determines the centrality dependence of nonflow two-particle correlations. Since the flow is known to vanish for central collisions by symmetry, one could measure (and then subtract) nonflow correlations by measuring them for central collisions and then assuming that they vary like  $1/N$ . Unfortunately, it is impossible to select ‘‘true’’ central collisions (with vanishing impact parameter) experimentally, so that this procedure may not be accurate.

Future heavy ion experiments at RHIC and LHC are likely to be affected in the same way by nonflow correlations. At these energies, directed flow is expected to be weaker than at SPS, maybe undetectable. On the other hand, elliptic flow should be at least of the same magnitude as at SPS. Pions should be used to determine the reaction plane since they are by far the most abundant. As the multiplicity



will be higher than at SPS, nonflow correlations will be smaller, since they are proportional to  $1/N$ . However, since the detectors will cover only a limited interval in rapidity, effects of  $\rho$  decays, HBT correlations and final state interactions may be important and should be taken into account in the measurement of the pion elliptic flow. Hard processes could give an additional contribution to nonflow correlations: there is a strong azimuthal correlation between jet fragments [43]. Clearly, more work is needed, both theoretical and experimental, in order to obtain accurate measurements of flow observables at ultrarelativistic energies. Alternative methods, based on multiparticle correlations, are currently under study [44].

### ACKNOWLEDGMENTS

We thank the Nuclear Theory group of Brookhaven National Laboratory for its hospitality during the period when

this work was done. We thank Terry Awes, Art Poskanzer, Hubertus Schlagheck, and Sergei Voloshin for detailed explanations concerning the NA49 and WA98 flow analyses, and Stefan Bass for discussions.

### APPENDIX A: CORRELATIONS FROM MOMENTUM CONSERVATION

We denote by  $\mathbf{p}_1, \dots, \mathbf{p}_N$  the momenta of the  $N$  particles emitted in a heavy ion collision and by  $\mathbf{p}_{T1}, \dots, \mathbf{p}_{TN}$  their transverse components. Since we are interested in azimuthal correlations, we consider only transverse momentum conservation:  $\mathbf{p}_{T1} + \dots + \mathbf{p}_{TN} = \mathbf{0}$ . We assume for simplicity that this is the only correlation between the momenta of the outgoing particles. We want to calculate the distribution of  $\mathbf{p}_1, \dots, \mathbf{p}_k$ , with  $k < N$ , defined as

$$f_c(\mathbf{p}_1, \dots, \mathbf{p}_k) \equiv \frac{\left( \prod_{i=1}^k f(\mathbf{p}_i) \right) \int \delta^2(\mathbf{p}_{T1} + \dots + \mathbf{p}_{TN}) \prod_{i=k+1}^N [f(\mathbf{p}_i) d^3 \mathbf{p}_i]}{\int \delta^2(\mathbf{p}_{T1} + \dots + \mathbf{p}_{TN}) \prod_{i=1}^N [f(\mathbf{p}_i) d^3 \mathbf{p}_i]}, \quad (\text{A1})$$

where  $f(\mathbf{p})$  denotes the single particle normalized transverse momentum distribution. The average transverse momentum is naturally assumed to be zero:

$$\langle \mathbf{p}_T \rangle \equiv \int \mathbf{p}_T f(\mathbf{p}) d^3 \mathbf{p} = \mathbf{0}. \quad (\text{A2})$$

In order to calculate the distribution  $f_c$  defined in Eq. (A1), we make use of the following lemma: the sum of  $M$  uncorrelated momenta  $\mathbf{P}_T \equiv \sum_{i=1}^M \mathbf{p}_{Ti}$  has a Gaussian distribution if  $M$  is large, according to the central limit theorem:

$$\begin{aligned} F_M(\mathbf{P}_T) &\equiv \int \delta^2\left(-\mathbf{P}_T + \sum_{i=1}^M \mathbf{p}_{Ti}\right) \prod_{i=1}^M [f(\mathbf{p}_i) d^3 \mathbf{p}_i] \\ &= \frac{1}{\pi \sigma^2} \exp\left(-\frac{\mathbf{P}_T^2}{\sigma^2}\right). \end{aligned} \quad (\text{A3})$$

In writing this equation, we have assumed that the transverse momentum distribution is isotropic in the transverse plane, i.e., we have neglected the azimuthal asymmetries (1), which are of the order of a few percent. The width of the Gaussian is

$$\sigma^2 = \langle \mathbf{P}_T^2 \rangle = M \langle p_T^2 \rangle. \quad (\text{A4})$$

Equations (A3) and (A4) allow us to write Eq. (A1) as

$$\begin{aligned} f_c(\mathbf{p}_1, \dots, \mathbf{p}_k) &= \left( \prod_{i=1}^k f(\mathbf{p}_i) \right) \frac{F_{N-k}\left(-\sum_{i=1}^k \mathbf{p}_{Ti}\right)}{F_N(\mathbf{0})} \\ &= \left( \prod_{i=1}^k f(\mathbf{p}_i) \right) \frac{N}{N-k} \exp\left(-\frac{\left(\sum_{i=1}^k \mathbf{p}_{Ti}\right)^2}{(N-k)\langle \mathbf{p}_T^2 \rangle}\right). \end{aligned} \quad (\text{A5})$$

For  $k=1$ , Eq. (A5) gives the corrected one-particle distribution

$$f_c(\mathbf{p}) = f(\mathbf{p}) \left( 1 + \frac{1}{N} - \frac{\mathbf{p}_T^2}{N \langle p_T^2 \rangle} \right), \quad (\text{A6})$$

where we have expanded the correction to leading order in  $1/N$ . Similarly, one obtains for  $k=2$

$$f_c(\mathbf{p}_1, \mathbf{p}_2) = f(\mathbf{p}_1) f(\mathbf{p}_2) \left( 1 + \frac{2}{N} - \frac{(\mathbf{p}_{T1} + \mathbf{p}_{T2})^2}{N \langle p_T^2 \rangle} \right). \quad (\text{A7})$$

The contribution of momentum conservation to the correlation function (3) is thus

$$C^{\Sigma p_T}(\mathbf{p}_1, \mathbf{p}_2) = \frac{f_c(\mathbf{p}_1, \mathbf{p}_2)}{f_c(\mathbf{p}_1) f_c(\mathbf{p}_2)} - 1 = -\frac{2 \mathbf{p}_{T1} \cdot \mathbf{p}_{T2}}{N \langle p_T^2 \rangle}. \quad (\text{A8})$$

Similar results were obtained in [18], Appendix B.

APPENDIX B: ESTIMATE OF  $\Sigma\langle p_T^2 \rangle$  AT SPS

In a central Pb-Pb collision at SPS, about 680 negatively charged particles are emitted [45]. If we assume that these are mostly  $\pi^-$  and  $K^-$  with a ratio  $\langle K^- \rangle / \langle \pi^- \rangle \sim 0.09$ , where  $\langle \pi \rangle \equiv (\langle \pi^+ \rangle + \langle \pi^- \rangle) / 2$  [26], there are some 625  $\pi^-$  and 55  $K^-$ . Taking into account the various kaon-to- $\pi$  ratios, as well as the expected isospin symmetry between pion species, this gives a total of 280 kaons and 1875 pions. With these particles come the 416 nucleons (we assume there is no fragment), giving about 2500 particles in all. We shall neglect the contributions to  $\Sigma\langle p_T^2 \rangle$  from other particles as, e.g., antiprotons.

In order to calculate the average value of the squared transverse momentum  $\langle p_T^2 \rangle$  for a particular particle species, one needs its distribution in transverse momentum and rapidity. The  $p_T$  and  $y$  dependences may factorize, leaving a normalized  $p_T$  distribution which is parametrized by

$$\frac{dN}{d^2\mathbf{p}_T} = \frac{e^{m/T}}{2\pi T(m+T)} \exp\left(-\frac{m_T}{T}\right), \quad (\text{B1})$$

where  $m_T = \sqrt{m^2 + p_T^2}$  is the transverse mass, while the inverse slope parameter  $T$  depends on the particle species and the energy of the collision. This parametrization can be used for the pions, nucleons, and kaons at SPS, with  $T_\pi = 180$  MeV,  $T_N = 300$  MeV, and  $T_K = 215$  MeV, respectively [45]. These numerical values fit transverse momentum spec-

tra in the central rapidity region. Away from midrapidity, transverse momenta are somewhat smaller, so that we overestimate  $\Sigma p_T^2$ . The spectrum (B1) yields an average  $\langle p_T^2 \rangle$  given by

$$\langle p_T^2 \rangle = 2mT \frac{1 + 3\frac{T}{m} + 3\frac{T^2}{m^2}}{1 + \frac{T}{m}}. \quad (\text{B2})$$

Substituting in Eq. (B2) the values of the inverse slope parameter  $T$  given above, and multiplying the resulting average squared transverse momentum by the multiplicity of the particle species, one obtains for a central collision at SPS

$$\sum_j \langle p_T^2 \rangle \sim 930 \text{ GeV}^2. \quad (\text{B3})$$

As mentioned above, this is somewhat overestimated since we have neglected the decrease of inverse slopes away from midrapidity.

For a noncentral collision, we assume that the sum of  $p_T^2$  scales with the multiplicity, i.e., we neglect the centrality dependence of inverse slopes and particle ratios. Therefore, in the case of semicentral collisions used by NA49 for flow studies, with only 40 to 55 % of the maximum multiplicity [9], the value (B3) must be divided by 2.

- 
- [1] J.-Y. Ollitrault, Phys. Rev. D **46**, 229 (1992).  
[2] P. Danielewicz *et al.*, Phys. Rev. Lett. **81**, 2438 (1998).  
[3] H. Heiselberg and A. M. Lévy, Phys. Rev. C **59**, 2716 (1999).  
[4] B. Zhang, M. Gyulassy, and C. M. Ko, Phys. Lett. B **455**, 45 (1999).  
[5] B. A. Li, C. M. Ko, A. T. Sustich, and B. Zhang, Phys. Rev. C **60**, 011901(R) (1999).  
[6] J. Barrette *et al.*, E877 Collaboration, Phys. Rev. C **59**, 884 (1999); **56**, 3254 (1997); **55**, 1420 (1997).  
[7] C. Pinkenburg *et al.*, E895 Collaboration, Phys. Rev. Lett. **83**, 1295 (1999).  
[8] D. J. Hofman for the E917 Collaboration, Nucl. Phys. **A661**, 75c (1999).  
[9] H. Appelshäuser *et al.*, NA49 Collaboration, Phys. Rev. Lett. **80**, 4136 (1998). The data we use in this paper are the revised data available on the NA49 web page <http://na49info.cern.ch/na49/Archives/Images/Publications/Phys.Rev.Lett.80:4136-4140,1998/>  
[10] M. M. Aggarwal *et al.*, WA98 Collaboration, nucl-ex/9807004.  
[11] M. M. Aggarwal *et al.*, WA98 Collaboration, Phys. Lett. B **469**, 30 (1999); T. Peitzmann for the WA98 Collaboration, Nucl. Phys. **A661**, 191c (1999); H. Schlagheck for the WA98 Collaboration, *ibid.* **A661**, 337c (1999); S. Nishimura for the WA98 Collaboration, *ibid.* **A661**, 464c (1999).  
[12] F. Ceretto for the CERES Collaboration, Nucl. Phys. **A638**, 467c (1998); B. Lenkeit for the CERES Collaboration, *ibid.* **A661**, 23c (1999).  
[13] S. Kabana for the NA52 Collaboration, Nucl. Phys. **A638**, 411c (1998).  
[14] P. Saturnini for the NA50 Collaboration, Nucl. Phys. **A661**, 345c (1999).  
[15] P. Danielewicz and G. Odyniec, Phys. Lett. **157B**, 146 (1985).  
[16] Note, however, that correlations between photons originating from  $\pi^0$  decays were considered in M. M. Aggarwal *et al.*, WA93 Collaboration, Phys. Lett. B **403**, 390 (1997).  
[17] P. M. Dinh, N. Borghini, and J.-Y. Ollitrault, Phys. Lett. B **477**, 51 (2000).  
[18] P. Danielewicz *et al.*, Phys. Rev. C **38**, 120 (1988).  
[19] S. Koonin, Phys. Lett. **70B**, 43 (1977); D. H. Boal, C.-K. Gelbke, and B. K. Jennings, Rev. Mod. Phys. **62**, 553 (1990).  
[20] H. Sorge, Phys. Rev. Lett. **82**, 2048 (1999).  
[21] S. A. Voloshin and A. M. Poskanzer, Phys. Lett. B **474**, 27 (2000).  
[22] L. V. Bravina, A. Faessler, C. Fuchs, and E. E. Zabrodin, Phys. Rev. C **61**, 064902 (2000).  
[23] S. A. Voloshin and Y. Zhang, Z. Phys. C **70**, 65 (1996).  
[24] For a review, see J.-Y. Ollitrault, Nucl. Phys. **A638**, 195c (1998).  
[25] M. M. Aggarwal *et al.*, WA98 Collaboration, Phys. Rev. Lett. **81**, 4087 (1998).  
[26] F. Siklér for the NA49 Collaboration, Nucl. Phys. **A661**, 45c (1999).  
[27] M. M. Aggarwal *et al.*, WA98 Collaboration, Phys. Lett. B **477**, 37 (2000).

- [28] S. A. Bass *et al.*, Prog. Part. Nucl. Phys. **41**, 225 (1998); S. A. Bass and A. Dumitru, Phys. Rev. C **61**, 064909 (2000).
- [29] G. Agakichiev *et al.*, CERES/TAPS Collaboration, Eur. Phys. J. C **4**, 231 (1998); **4**, 249 (1998).
- [30] Y. Pang, Nucl. Phys. **A638**, 219c (1998).
- [31] J. Stachel, Nucl. Phys. **A654**, 119c (1999).
- [32] S. Mrówczyński, nucl-th/9907099.
- [33] R. Ganz, NA49 Collaboration, Nucl. Phys. **A661**, 448c (1999).
- [34] K. Kaimi *et al.*, NA44 Collaboration, Z. Phys. C **75**, 619 (1997).
- [35] W. Bauer, C. Gelbke, and S. Pratt, Annu. Rev. Nucl. Part. Sci. **42**, 77 (1992), and references therein.
- [36] R. Lednicky, “NA49 Results on unlike particle correlations,” NA49 note 210, 11/11/99.
- [37] A. M. Poskanzer (private communication).
- [38] S. A. Bass *et al.*, Phys. Lett. B **302**, 381 (1993); Phys. Rev. C **51**, 3343 (1995); S. Soff *et al.*, nucl-th/9903061.
- [39] B.-A. Li, Nucl. Phys. **A570**, 797 (1994).
- [40] A. M. Poskanzer and S. A. Voloshin, NA49 Collaboration, Nucl. Phys. **A661**, 341c (1999).
- [41] S. Nishimura, WA98 Collaboration, Nucl. Phys. **A638**, 459c (1998); H. Schlagheck, Ph.D. thesis, Universität Münster, 1998.
- [42] H. Appelshäuser *et al.*, NA49 Collaboration, Phys. Lett. B **467**, 21 (1999).
- [43] A. Leonidov and J.-Y. Ollitrault (in preparation).
- [44] N. Borghini, P. M. Dinh, and J.-Y. Ollitrault, nucl-th/0007063 (submitted to Phys. Rev. C).
- [45] P. Jacobs, NA49 Collaboration, in *Physics and Astrophysics of Quark-Gluon Plasma*, edited by B. C. Sinha, D. K. Srivastava, and Y. P. Viyogi (Narosa Publishing House, New Delhi, 1998), p. 248.